

Double-Pass Flat-Plate Solar Air Heaters with External Recycle

C. D. Ho*, R. C. Wang and T. C. Chen

Department of Chemical and Materials Engineering, Tamkang University, Tamsui 251, Taipei, Taiwan

Abstract

A new device of inserting an absorbing plate to divide a flat-plate channel into two channels with fins attached and external recycling at the ends, resulting in substantially improving the heat transfer efficiency, has been investigated both experimentally and theoretically. The agreement of the theoretical predictions with those measured values from the experimental results is fairly good. The experimental and theoretical results are represented graphically and compared with that in the downward-type single-pass solar air heaters of the same size without recycling. Considerable improvement in heat transfer is obtained by employing double-pass operations with external recycling and fin attached over and under the absorbing plate. The influences of recycle ratio and absorbing plate location on the heat-transfer efficiency enhancement as well as on the power consumption increment have been also delineated

Keywords: Solar air heaters; flat-plate type; double-pass operations; collector efficiency.

1. Introduction

Flat-plate solar collectors which absorb the solar radiation, transform it into heat, and to heat passing air are mechanically simpler than concentrating collectors to be used in domestic and industrial needs. The flat-plate solar air heaters are constructed with the blackened absorber to transfer the absorbed energy to the flowing medium, transparent cover to reduce convection and radiation losses to atmosphere, and back and side insulation to reduce conduction losses. The main application of solar air heaters are space heating (Joudi and Dhaidan, 2001) and drying (Yaldyz and Ertekyn, 2001). The recycle-effect concept in double- and multi-pass operation for creating the turbulence of air flowing can effectively enhance the heat transfer rate and lead to improved device performance (Ho et al., 2001; Ho and Yang, 2003). Moreover, the design of double-pass device and attaching the fins to the absorber plate are to extend the heat transfer area, resulting in the collector efficiency enhancement. An

alternative design device for improving collector efficiency by increasing heat transfer coefficient has been studied with experiment and theoretical predictions.

2. Theory

The double-pass solar air heater with fins attached of channel width W , channel length L , and height of both upper and lower channels H , may be illustrated by the schematic diagram of Fig. 1 with artificial simulation. The total heat flow from the absorber plate with attaching fins to a passing airflow may be written as

$$q' = h_1 \left(A_i + A_f \tanh m_f H_f / m_f H_f \right) (T_p - T_i(z)), i = a, b \quad (1)$$

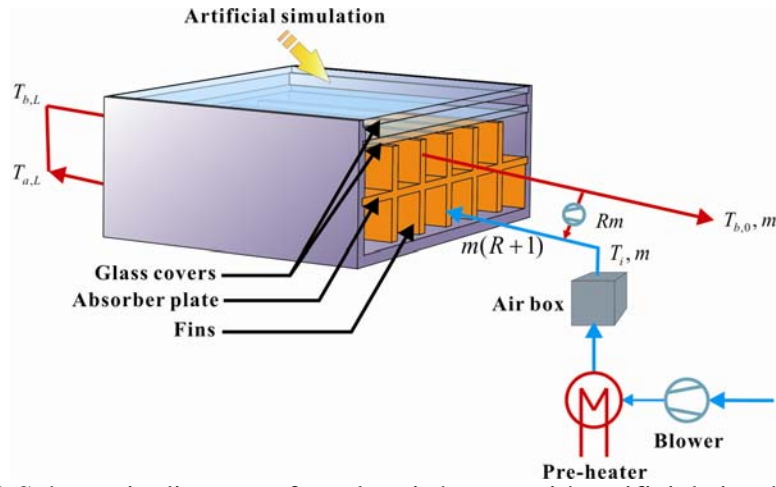


Fig.1 Schematic diagram of a solar air heater with artificial simulation.

Basing on the concept of energy conservation, the temperature distributions for lower and upper channels are similar to that presented in our previous work with the same working dimensions (Ho et al., 2005), except that the correlation coefficient of heat transfer rate ϕ_1 and ϕ_2 in Eqs. (30) and (31) of **Appendix**, respectively, are estimated for the device with fins attached as follows:

$$T_a(\xi) = \frac{Y_1 - B_5}{B_4} C_1 e^{Y_1 \xi} + \frac{Y_2 - B_5}{B_4} C_2 e^{Y_2 \xi} - \frac{B_5(B_3 B_4 - B_1 B_6)}{B_4(B_1 B_5 - B_2 B_4)} - \frac{B_6}{B_4} + T_s \quad (2)$$

$$T_b(\xi) = C_1 e^{Y_1 \xi} + C_2 e^{Y_2 \xi} + \frac{B_3 B_4 - B_1 B_6}{B_1 B_5 - B_2 B_4} + T_s \quad (3)$$

where

$$Y_1 = \frac{(B_1 + B_5) + \sqrt{(B_1 - B_5)^2 + 4B_2 B_4}}{2} \quad (4)$$

$$Y_2 = \frac{(B_1 + B_5) - \sqrt{(B_1 - B_5)^2 + 4B_2 B_4}}{2} \quad (5)$$

$$C_1 = \left[\frac{F_2 H_2 R - F_2 (I_2 + H_2 R) e^{Y_2} - (F_2 + F_3) B_4}{F_1 [(I_2 + H_2 R) e^{Y_2} - (I_1 + H_1 R) e^{Y_1} + (H_1 - H_2) R]} \right] \quad (6)$$

and

flow rate Rm which is regulated with the aid of a blower and a valve situated at the exiting of the upper subchannel. The air temperatures at the inlet and outlet of the solar collector, ambient temperature, temperature of the absorber plate and the mass flow rate were measured with probes. The designing and operating parameters employed in this work are as follows: $A_c = 0.09 \text{ m}^2$, $H = 0.05 \text{ m}$, $h_B = h_f = 0.05 \text{ m}$, $k_B = 4.68 \times 10^{-2} \text{ kJ/kg K}$, $k_f = 4.68 \times 10^{-2} \text{ kJ/kg K}$, $k_s = 125 \times 10^{-4} \text{ kJ/kg K}$, $L = 0.3 \text{ m}$, $l = 0.12 \text{ m}$, $l_B = l_s = 0.06 \text{ m}$, $T_{in} = 30 \text{ }^\circ\text{C}$, $T_s = 30 \text{ }^\circ\text{C}$, $t_f = 0.002 \text{ m}$, $V = 1.0 \text{ m/s}$, $W = 0.3 \text{ m}$, $W_B = 0.03 \text{ m}$, $\alpha_p = 0.96$, $\varepsilon_p = 0.8$, $\varepsilon_R = 0.94$, $\tau_g = 0.875$.

4. Results and discussion

The theoretical predictions and experimental results of collector efficiencies for the double-pass solar air heater with external recycle and fins attached have been carried out as shown in Figs. 3 and 4. The collector efficiencies increase with increasing recycle ratio and air mass flow rate. There are two conflict effects in the recyclic device, the desirable effect of increasing convective heat-transfer coefficient due to the increasing air velocity and undesirable effect of reducing heat-transfer driving force owing to the premixing effect at the inlet as compared that to the single-pass device. In the present study, however, the desirable effect is a predominant factor and can compensate for the decrease of the temperature driving force.

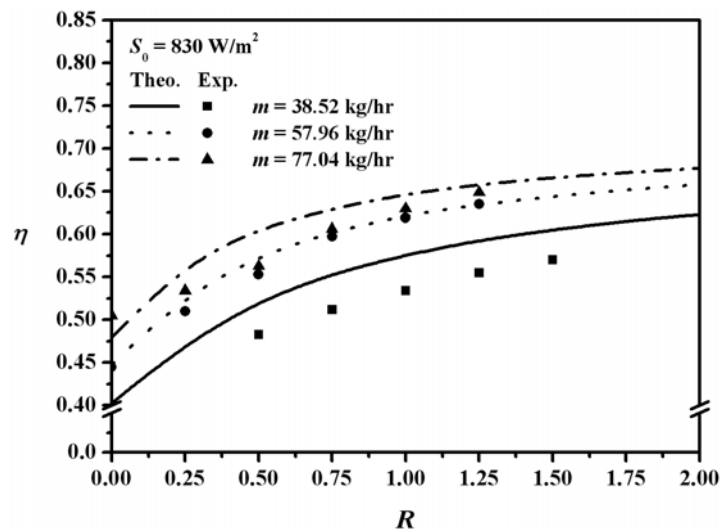


Fig. 3 Effect of recycle ratio on collector efficiency of air with air mass flow rate as parameter, $S_0 = 830 \text{ W/m}^2$.

The comparison of collector efficiencies between the devices with recycle and the one of single-pass operation without recycle is readily observed from Table 1. The theoretical predictions show that the collector efficiency improvement increases with increasing recycle ratio and incident solar radiation but with decreasing mass flow rate. It is seen from Table 1 that the recycle double-pass solar air heater with fins attached has good performance in the heat transfer rate.

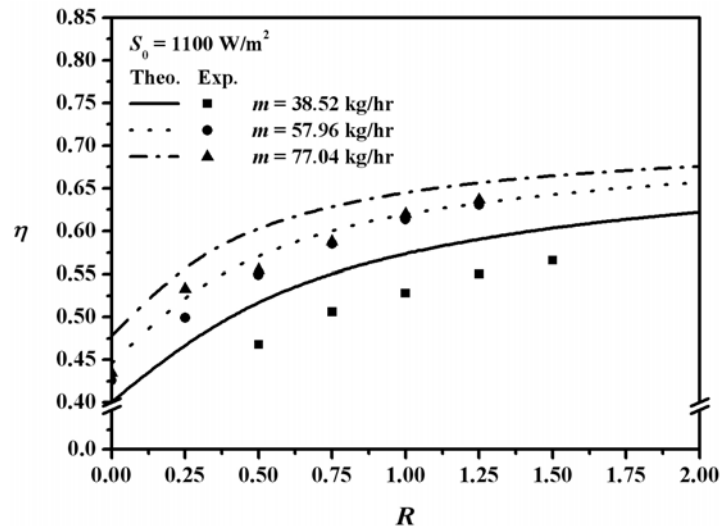


Fig. 4 Effect of recycle ratio on collector efficiency of air with air mass flow rate as parameter, $S_0 = 1100 \text{ W/m}^2$.

Table 1 The collector efficiency improvement of solar air heaters

| I_D (%) | $S_0 = 830 \text{ W/m}^2$ (Theo.) | | | $S_0 = 830 \text{ W/m}^2$ (Exp.) | | |
|---------------------------|------------------------------------|-----------|-----------|-----------------------------------|-----------|-----------|
| | $R = 0$ | $R = 0.5$ | $R = 1.0$ | $R = 0$ | $R = 0.5$ | $R = 1.0$ |
| $m = 38.52 \text{ kg/hr}$ | 30.42 | 68.93 | 86.41 | 13.27 | 56.31 | 72.82 |
| $m = 57.96 \text{ kg/hr}$ | 21.08 | 55.41 | 68.11 | 20.27 | 49.46 | 67.30 |
| $m = 77.04 \text{ kg/hr}$ | 15.70 | 46.62 | 56.28 | 21.98 | 35.99 | 52.17 |
| | $S_0 = 1100 \text{ W/m}^2$ (Theo.) | | | $S_0 = 1100 \text{ W/m}^2$ (Exp.) | | |
| $m = 38.52 \text{ kg/hr}$ | 30.19 | 68.83 | 86.69 | 10.71 | 51.95 | 71.43 |
| $m = 57.96 \text{ kg/hr}$ | 20.87 | 55.56 | 68.29 | 15.45 | 48.78 | 66.40 |
| $m = 77.04 \text{ kg/hr}$ | 17.16 | 48.53 | 58.33 | 6.62 | 36.03 | 51.96 |

Figure 5 presents the influence of recycle ratio on the real collector efficiency improvement with air mass flow rate as a parameter. The real collector efficiency improvement is an index factor to know how to operate in suitable conditions. Although the higher mass flow rate of air and recycle ratio are useful to increase the heat transfer coefficient resulting in the collector efficiency enhancement, the undesirable accompaniment, say the hydraulic dissipated energy, increases accordingly. There exists an optimum recycle ratio in recycle double-pass solar air heaters under high mass flow rate of air and low blower efficiency. This paper provides the valuable results for designing such solar air heaters under recycle operations.

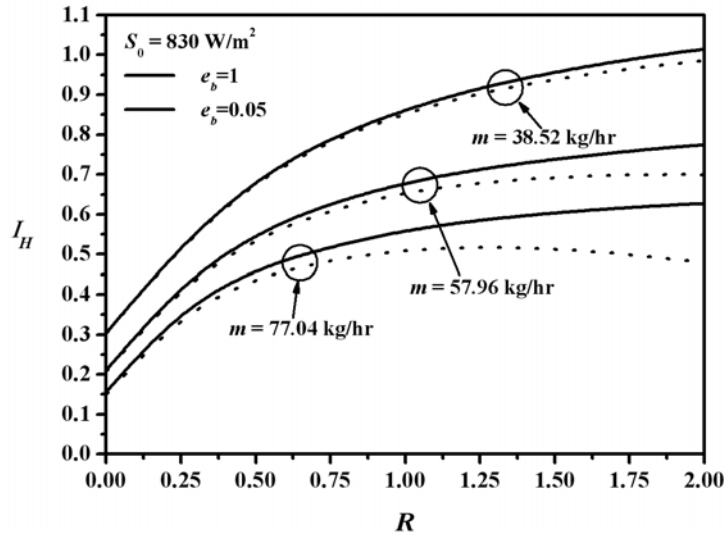


Fig. 5 Effect of recycle ratio on real collector efficiency improvement with air mass flow rate as parameter, $S_0 = 830 \text{ W/m}^2$.

References

- Ho, C. D., Yeh H. M. and Chiang S. C., (2001) *Industrial and Engineering Chemistry Research*, 40, 5839-5846.
- Ho, C. D. Yeh H. M. and Wang R. C., (2005) *Energy*, 30, 2796-2817.
- Ho, C. D. and Yang W. Y., (2003) *Chemical Engineering Science*, 58, 1235-1250.
- Joudi, K. A. and Dhaidan, N. S., (2001) *Energy Conversion and Management*, 42, 995-1022.
- Yaldyz, O. and Ertekyn, C., (2001) *Drying Technology*, 19, 583-597.

Acknowledgements

The authors wish to thank the National Science Council of the Republic of China for its financial support

Appendix

$$G_1 = (\phi_2 h_2 + U_T + U_B) / (U_T + U_B + \phi_1 h_1 + \phi_2 h_2) \quad (14)$$

$$G_2 = \phi_2 h_2 / (U_T + U_B + \phi_1 h_1 + \phi_2 h_2) \quad (15)$$

$$G_3 = S_0 a_p \tau_g^2 / (U_T + U_B + \phi_1 h_1 + \phi_2 h_2) \quad (16)$$

$$G_4 = (h_{r,p-c_1} + h_1 + U_{c_1-s})^{-1} \quad (17)$$

$$G_5 = (\phi_1 h_1 + U_T + U_B) / (U_T + U_B + \phi_1 h_1 + \phi_2 h_2) \quad (18)$$

$$G_6 = h_1 / (U_T + U_B + \phi_1 h_1 + \phi_2 h_2) \quad (19)$$

$$G_7 = (h_{r,p-R} + h_2 + U_{B-s})^{-1} \quad (20)$$

$$B_1 = (-h_{r,p-c_1} h_1 G_3 G_4 - h_1 \phi_1 G_3 - U_{c_1-s} h_1 G_4) / M_1 \quad (21)$$

$$B_2 = (h_1 \phi_1 G_2 + h_{r,p-c_1} h_1 G_2 G_4) / M_1 \quad (22)$$

$$B_3 = (h_1 \phi_1 G_3 + h_{r,p-c_1} h_1 G_3 G_4) / M_1 \quad (23)$$

$$B_4 = (h_2 \phi_2 G_6 + h_{r,p-R} h_2 G_6 G_7) / M_2 \quad (24)$$

$$B_5 = (-h_{r,p-R} h_2 G_5 G_7 - h_2 \phi_2 G_5 - U_{B-s} h_2 G_7) / M_2 \quad (25)$$

$$B_6 = (h_2 \phi_2 G_3 + h_{r,p-R} h_2 G_3 G_7) / M_2 \quad (26)$$

$$M_1 = \left[\frac{-m(1+R)C_p}{WL} \right] = -m(1+R)C_p / A_c \quad (27)$$

$$M_2 = \left[\frac{m(1+R)C_p}{WL} \right] = m(1+R)C_p / A_c \quad (28)$$

$$\xi = z / L \quad (29)$$

$$\phi_1 = 1 + \frac{A_{f,1}}{A_t} \eta_{f,1} \quad (30)$$

$$\phi_2 = 1 + \frac{A_{f,2}}{A_t} \eta_{f,2} \quad (31)$$

$$F_1 = B_1 B_5 - B_2 B_4 \quad (32)$$

$$F_2 = B_3 B_4 - B_1 B_6 \quad (33)$$

$$F_3 = B_3 B_5 - B_2 B_6 \quad (34)$$

$$I_1 = Y_1 - B_4 - B_5 \quad (35)$$

$$I_2 = Y_2 - B_4 - B_5 \quad (36)$$

$$H_1 = Y_1 - D_5 \quad (37)$$

$$H_2 = Y_2 - D_5 \quad (38)$$

Nomenclature

| | |
|-----------------------|--|
| A_c | surface area of the collector = LW (m^2) |
| A_f | total surface area of attached fins (m) |
| A_t | the area of absorber plate less the welded area of fins (m) |
| B | coefficients defined Eqs. (29)-(34) |
| C_p | specific heat of air at constant pressure (kJ/kg K) |
| $D_{e,0}$, | equivalent diameter of downward-type single-pass device, lower |
| $D_{e,a}$, $D_{e,b}$ | channel and upper channel of solar air heaters, respectively (m) |
| e_b | blower efficiency |

| | |
|-------------------|--|
| F | coefficients defined Eqs. (32)-(34) |
| f_F | Fanning friction factor |
| H | height of upper and lower channel (m) |
| H_1, H_2 | coefficients defined Eqs. (49) and (50) |
| H_T | the hydraulic dissipated energy increment (W) |
| H_f | height of fins (m) |
| h_i | heat-transfer coefficient of air (kJ/s m ² K) |
| h_r | radiative heat-transfer coefficient between two parallel plates (kJ/s m ² K) |
| h_{r,c_1-c_2} , | radiation heat transfer coefficients defined Eqs. (65)-(68) (kJ/s m ² K) |
| h_{r,c_2-s} , | |
| $h_{r,p-c_1}$, | |
| $h_{r,p-R}$ | |
| I | coefficients defined Eqs. (35) and (36) |
| I_D | percentage of collector efficiency improvement, defined by Eq. (9) |
| I_H | real collector efficiency improvement |
| $k, k_B,$ | thermal conductivity of air, bottom plate, fins and insulator, respectively |
| k_f, k_s | (kJ/s m K) |
| L | channel length (m) |
| l_B, l_s | thickness of the bottom plate and insulator, respectively (m) |
| m | the total air mass flow rate (kg/hr) |
| m_f | coefficient defined as $m_f = \sqrt{2h_i(L + t_f) / k_f A_{ff}}$ |
| M_1, M_2 | coefficients defined Eqs. (27) and (28) |
| $Q_u, Q_{u,D}$ | useful energy gain carried away by air per unit time of double-pass and downward type solar air heaters, respectively (kJ/s) |
| q' | total heat flow from solar collector to a passing air flow (kJ/s) |
| R | recycle ratio |
| S_0 | incident solar radiation (kJ/s m ²) |
| T_i | inlet temperature (K) |
| $T_a(z)$ | fluid temperature in lower channel (K) |
| $T_b(z)$ | fluid temperature in upper channel (K) |
| T_p | temperature of the absorber plate (K) |
| T_s | ambient temperature (K) |
| t_f | thickness of fins (m) |
| U_B | loss coefficient from the bottom of solar air heater to the ambient (kJ/s |

| | |
|--|--|
| | $\text{m}^2 \text{ K}$) |
| U_{B-s} | loss coefficient from the surfaces of edges and the bottom of the solar collector to the ambient ($\text{kJ/s m}^2 \text{ K}$) |
| U_{c_1-s} | loss coefficient from the glass cover to the ambient ($\text{kJ/s m}^2 \text{ K}$) |
| U_T | loss coefficient from the top of solar air heater to the ambient ($\text{kJ/s m}^2 \text{ K}$) |
| W | both upper and lower channel widths (m) |
| $\overline{v_0}, \overline{v_a}, \overline{v_b}$ | average air velocity in the downward-type single-pass device, lower channel and upper channel of solar air heaters, (m/s) |
| V | wind velocity (m/s) |
| z | axial coordinate along the flow direction (m) |
| α_p | absorptivity of the absorber plate |
| η, η_D | the collector efficiencies of double-pass type and downward-type single-pass solar air heater, respectively |
| η_f | fin efficiency defined as $\eta_f = \tanh m_f H_f / m_f H_f$ |
| τ_g | transmittance of the glass cover |
| ρ | air density (kg/m^3) |
| ξ | dimensionless of channel length defined Eq. (37) |
| ϕ | correlation coefficient of heat transfer rate defined Eqs. (30) and (31) |